Title

Front propagation and critical gradient transport models

Journal

Physics of Plasmas, 14(12)

ISSN

1070-664X

Authors

Garbet, X
Sarazin, Y
Imbeaux, F
et al.

Publication Date

2007-12-01

DOI

10.1063/1.2824375

Front propagation and critical gradient transport models

X. Garbet, Y. Sarazin, F. Imbeaux, P. Ghendrih, and C. Bourdelle
Association Euratom-CEA, CEA/DSM/DRFC, CEA-Cadarache, 13108 Saint Paul Lez Durance, France

Ö. D. Gürcan and P. H. Diamond
Center for Astrophysics and Space Sciences, University of California San Diego, La Jolla, California 92093-0319, USA

(Received 17 September 2007; accepted 9 November 2007; published online 26 December 2007)

This paper analyzes the properties of a two-field critical gradient model that couples a heat equation to an evolution equation for the turbulence intensity. It is shown that the dynamics of a perturbation is ballistic or diffusive depending on the shape of the pulse and also on the distance of the temperature gradient to the instability threshold. This dual character appears in the linear response of this model for a wave packet. It is recovered when investigating the nonlinear solutions of this system. Both self-similar diffusive fronts and ballistic fronts are shown to exist. When the propagation is ballistic, it is found that the front velocity is the geometric mean between the turbulent diffusion coefficient and a microinstability growth rate. © *2007 American Institute of Physics*. [DOI: 10.1063/1.2824375]

I. INTRODUCTION

The development of a mean field theory of turbulent transport has long been a subject of interest in plasma physics. In particular, it provides the basis for writing reduced transport models for fusion plasmas, which allow us to calculate at low cost the mean density, velocity, and temperature profiles. Models based on a quasilinear theory coupled to a mixing length estimate have met some success in the past.[1,2] Nevertheless reduced transport models sometimes fail,[3] for reasons which are not always easy to identify. This is the reason why semiheuristic models such as Critical Gradient Models (CGM) (Refs. 5 and 6) have been developed, in particular for interpreting modulation experiments (see Ref. 4 for an overview). Their main advantage is the handling of a limited number of free parameters, which are deduced from experiment and can be compared in different devices. This procedure has been quite successful in analyzing modulation experiments,[7] and is supported by recent comparison between experiment and theory on AUG.[8] However it was shown recently that a Critical Gradient Model fails to explain the fast propagation of a cold pulse produced by impurity laser blow-off and the dynamics of the electron temperature during heat modulation, when using the same set of parameters. These two experiments were done simultaneously in the same discharges on JET, to minimize the sources of errors.[9] Hence it appears that the same plasma can exhibit a slow quasidiffusive or a fast ballistic-like behavior, depending on the type of transient that is performed. This is quite a challenge for theory.

Several attempts have been proposed to solve this issue, and to improve the reliability of transport predictions. Intermittency is often invoked as the main argument against the development of a mean field theory based on a combination of quasilinear and mixing-length theories. The reason is that intermittency contradicts the assumption of Gaussian statistics, which underlies most closure schemes used for justifying the quasilinear theory or the use of a mixing-length estimate. Models based on fractional kinetics have been proposed to overcome this difficulty.[10] These models are able to exhibit both diffusive and ballistic behaviors. They are however quite delicate to deal with in practice. Moreover they are usually considered in the test-particle limit, i.e., for a given statistics of fluctuations, whereas one would like to incorporate a self-consistent relation between the turbulence intensity and the gradients which drive the fluctuations. So an interesting question is whether a more "conventional" model based on a set of partial derivative equations is sufficient to describe the whole dynamics. One purpose of this paper is to show that a mean field model can be double-faced, i.e., diffusive in some cases, and ballistic in others. Certainly the simplest critical gradient model cannot do that. However it can be modified to exhibit such a bivalent character. The basic idea is to couple the transport equation to an evolution equation for the turbulence intensity, i.e., to deal with a two-field critical gradient model. This is not a new idea by far. Similar models have been proposed for modeling the dynamics of barrier formation,[11–13] avalanche dynamics,[14] self-organized critical systems,[15] and turbulence spreading.[16–20] The model proposed by Naulin *et al.*[19] was compared quite successfully to JET experimental data.[21] The model that is presented here is kind of minimal, ignoring in particular the possible role of a group velocity,[20,22] which may obviously drive a ballistic behavior. Also it does not account for shear flows (mean or zonal flows), which are important players in the dynamics of transport transients. This is particularly obvious when a transport event crosses a transport barrier.

The main aim of the paper is to derive some exact results related to this class of models. It is shown in particular that the system linear response exhibits a diffusive or a ballistic dynamics depending on parameters such as the heat flux and the wave number. This dual character is also revealed when investigating the nonlinear solutions of this system. Self-similar diffusive fronts and ballistic fronts are shown to exist,

thus extending previous results by Hahm *et al.*[16] for self-similar fronts, and by Gürcan and Diamond for ballistic fronts.[23] The existence of these nonlinear front solutions indicate that the double character of a two-field critical gradient model is a robust feature.

The paper is organized as follows: The coupling between a critical gradient model and an evolution equation for turbulence intensity is described in Sec. II. The linear response for a heat wave is described in Sec. III. Nonlinear solutions are investigated in a second stage: self-similar solutions are presented in Sec. IV and ballistic fronts in Sec. V. The main results are summarized in Sec. VI, together with a tentative explanation for some of the puzzling behaviors observed in experiments. A conclusion follows.

II. TWO-FIELD CRITICAL GRADIENT MODEL

A. Formulation

We consider here a simple slab geometry and a heat equation coupled to an evolution equation for the level of fluctuations

$$\partial_t T = D_0 \partial_x (E \partial_x T) + D_c \partial_{xx} T + S, \tag{1}$$

$$\partial_t E = \gamma_0 (\partial_x T - \kappa_c) \Upsilon (\partial_x T - \kappa_c) E - \gamma_{nl} E^2 + D_1 \partial_x (E \partial_x E). \tag{2}$$

Here, T is the temperature, and E represents a dimensionless turbulence intensity. Typically in a tokamak, E would be the square of electric potential fluctuations normalized to the mixing length level, so that $E \simeq 1$ in usual conditions. Here the coordinate x ranges between 0 and the system size a. The rate $\gamma_0 \kappa_c$ is representative of a linear growth rate, and γ_{nl} is an effective dissipation rate that leads to saturation due to mode coupling. It is expected that $\gamma_{nl} \simeq \gamma_0 \kappa_c$, consistently with a saturated level $E \simeq 1$. The turbulent diffusion coefficients D_0 and D_1 are of the same order of magnitude, as the underlying mechanisms are the same, i.e., nonlinear mode-mode coupling.[20,22] While D_0 is associated with heat transport, the coefficient D_1 measures the effect of turbulence spreading. This term is nonlocal in essence, in contrast to the quadratic saturation term [second term in the r.h.s. of Eq. (2)], which is purely local. The collisional diffusion coefficient D_c is much smaller than D_0 and D_1. For the sake of simplicity, we will assume $D_c = 0$ throughout this paper. In a tokamak, $\gamma_0 \kappa_c$, and therefore γ_{nl}, ranges between a few 10^4 and 10^5 s^{-1}, and $D_0 \approx 1$ m^2 s^{-1}. The model Eqs. (1) and (2) bears some similarities with the one proposed by Naulin *et al.*[19] One difference is that the turbulent transport vanishes below the critical threshold in the present model, whereas it becomes negative (heat pinch) in Naulin's model. Also the expression of the turbulent flux is somewhat different. The present model is also quite close to the one proposed by Gürcan and Diamond,[20] although group velocity effects were accounted for in the later work, while they are ignored here. The inclusion of a group velocity would obviously offer an additional possibility for ballistic behavior. The parameter κ_c is a stability threshold. This is an important ingredient of the model as this kind of system is prone to relaxations towards the stability threshold (profile stiffness). Profile relaxation is also the mechanism that underlies avalanches, i.e., transport events which propagate due to the interplay between profile and fluctuations.[24–27] It will be seen that there is indeed a close connection between avalanches and ballistic fronts. To simplify the notations, we will omit writing explicitly the Heaviside function $\Upsilon(\partial_x T - \kappa_c)$, being understood that solutions are verified to be supercritical. The boundary conditions are $T=0$ at $x=0$, and $\partial_x T = 0$ at $x=a$. The function S is a heat source normalized to the density, which is written as $S = D_0 \Phi \delta(x-a)$, where Φ is positive and constant, and scales as a temperature gradient. In other words we assume a constant thermal flux (when applied to a tokamak geometry, $x=0$ would be the edge and $x=a$ the magnetic axis, a the minor radius). Ignoring turbulence spreading (i.e., $D_1 = 0$), and assuming that the instability growth time is much smaller than the confinement time so that the turbulence intensity E is enslaved to the temperature gradient $\partial_x T$, one finds that at each time the turbulence intensity is given by the relation

$$E = \frac{1}{g} (\partial_x T - \kappa_c) \Upsilon (\partial_x T - \kappa_c), \tag{3}$$

where $g = \gamma_{nl} / \gamma_0$. The turbulent heat diffusivity is of the form

$$D_{\text{turb}} = \frac{D_0}{g} (\partial_x T - \kappa_c) \Upsilon (\partial_x T - \kappa_c) \tag{4}$$

so that the traditional Critical Gradient Model is recovered. In the following, it is shown that there exists cases where this scale separation assumption is not justified. Given the restrictions above, the system Eqs. (1) and (2) reads

$$\partial_t T = D_0 \partial_x [E \partial_x T + \Phi \Upsilon (x-1)], \tag{5}$$

$$\partial_t E = \gamma_0 (\partial_x T - \kappa_c) E - \gamma_{nl} E^2 + D_1 \partial_x (E \partial_x E). \tag{6}$$

A useful equivalent form of Eqs. (5) and (6), is obtained by taking the first derivative of the transport equation and by replacing the temperature by its gradient $A = \partial_x T$. The resulting system is

$$\partial_t A = D_0 \partial_{xx} [EA + \Phi \Upsilon (x-1)], \tag{7}$$

$$\partial_t E = \gamma_0 (A - \kappa_c) E - \gamma_{nl} E^2 + D_1 \partial_x (E \partial_x E). \tag{8}$$

B. Steady-state solution

Ignoring momentarily the turbulence spreading term, one finds that the steady state solution is given by Eq. (3) and therefore, for $x < a$,

$$A(A - \kappa_c) - g\Phi = 0. \tag{9}$$

The solution above the threshold is

$$A_0 = \frac{\kappa_c}{2} + \sqrt{\frac{\kappa_c^2}{4} + g\Phi} \tag{10}$$

and the corresponding turbulence intensity

$$E_0 = \frac{1}{g}\left(-\frac{\kappa_c}{2} + \sqrt{\frac{\kappa_c^2}{4} + g\Phi}\right). \tag{11}$$

The solution with spreading remains the same for constant flux Φ and threshold κ_c. Indeed adding a diffusion does not affect constant profiles in a homogenous medium. For nonconstant parameters, explicit solutions do not exist. Solutions were found however[16,17] in the special case where the growth rate is piecewise constant (i.e., here for constant temperature gradient). Also approximate analytical solutions were produced by Waltz and Candy,[18] which illustrate the nonlocal character of transport models that incorporate turbulence spreading.

III. PROPAGATION OF SMALL AMPLITUDE PERTURBATION

A. Linear dispersion relation

We now investigate the propagation of small amplitude perturbations, with arbitrary shape. This is useful in view of the weak transport transients produced for instance by low power heat modulation. Also it provides some insight into the dynamics of nonlinear ballistic fronts. The perturbations $\tilde{A}=A-A_0$ and $\tilde{E}=E-E_0$ are supposed to be small enough for the transport Eqs. (7) and (8) to be linearized. We consider the equilibrium given by Eqs. (10) and (11), which corresponds to constant background gradient A_0 and turbulence intensity E_0. An efficient way for solving this problem is to write the perturbation as a Fourier integral (typically a wave packet)

$$\tilde{A}(x,t) = \int_{-\infty}^{+\infty} \frac{dk}{2\pi} \tilde{A}_k e^{i(kx-\omega t)},$$
$$\tilde{E}(x,t) = \int_{-\infty}^{+\infty} \frac{dk}{2\pi} \tilde{E}_k e^{i(kx-\omega t)} \tag{12}$$

and to follow the propagation for each Fourier component. One finds the following response for a wave number k and a pulsation ω,

$$(i\omega - \mathcal{D}_0 k^2)\tilde{A}_k - D_0 A_0 k^2 \tilde{E}_k = 0, \tag{13}$$

$$\gamma_0 E_0 \tilde{A}_k + (i\omega + \gamma - \mathcal{D}_1 k^2)\tilde{E}_k = 0, \tag{14}$$

where $\gamma = \gamma_0(A_0-\kappa_c) - 2\gamma_{nl}E_0$, $\mathcal{D}_0 = D_0 E_0$, and $\mathcal{D}_1 = D_1 E_0$. The dispersion relation for a thermal wave is then easily calculated

$$\omega^2 + i[(\mathcal{D}_0 + \mathcal{D}_1)k^2 - \gamma]\omega - k^2 v_f^2 - \mathcal{D}_0 k^2(\mathcal{D}_1 k^2 - \gamma) = 0. \tag{15}$$

This equation admits two roots

$$\omega_\pm = -\frac{i}{2}[(\mathcal{D}_0 + \mathcal{D}_1)k^2 - \gamma] \pm \left\{k^2 v_f^2 + \frac{1}{4}[(\mathcal{D}_0 - \mathcal{D}_1)k^2 + \gamma]^2\right\}^{1/2} \tag{16}$$

where the velocity v_f is given by the relation,

$$v_f = (D_0 \gamma_0 A_0 E_0)^{1/2}. \tag{17}$$

An alternative expression is found when using the explicit expression of the steady solution Eqs. (10) and (11), namely $v_f = (D_0\gamma_0\Phi)^{1/2}$. Also it is stressed that for this fixed point, $\gamma = -\gamma_{nl}E_0$ is negative.

B. Diffusion versus ballistic behavior

Two limit cases can be identified from the solution Eq. (16).

Case 1: $[(\mathcal{D}_1-\mathcal{D}_0)k^2-\gamma]^2 \gg 4k^2 v_f^2$.

One finds two damped thermal waves

$$\omega_+ = -i(\mathcal{D}_1 k^2 - \gamma), \tag{18}$$

$$\omega_- = -i\mathcal{D}_0 k^2. \tag{19}$$

These solutions correspond to the usual damped diffusive waves (be reminded here that γ is negative).

Case 2: $[(\mathcal{D}_1-\mathcal{D}_0)k^2-\gamma]^2 \ll 4k^2 v_f^2$. In this case, two ballistic co- and counterpropagating waves are found

$$\omega_\pm = \pm k v_f. \tag{20}$$

The condition for moving from a diffusive to a ballistic response can be recast as a condition on the thermal flux Φ. The dynamics for a given wave number is ballistic when the flux Φ is much lower than the critical value

$$\Phi_c = \kappa_c^2 \frac{4\gamma_0 D_0 k^2 [(D_1 - D_0)k^2 - \gamma_{nl}]^2}{\{[(D_1 - D_0)k^2 - \gamma_{nl}]^2 - 4\gamma_{nl} D_0 k^2\}^2}. \tag{21}$$

For a wave number that is smaller than the inverse of the turbulence correlation length (i.e., $k\ell \leq 1$, where ℓ is a turbulence correlation length), one gets the condition $\gamma_0\kappa_c, \gamma_{nl} \gg (D_0+D_1)k^2$ since the spreading diffusion is of the same order as the heat diffusivity, i.e., $D_0 \simeq D_1 \simeq 1\ \mathrm{m^2\ s^{-1}}$, and the growth rate $\gamma_0 \simeq \gamma_{nl} \simeq 10^5\ \mathrm{s^{-1}}$. In this case, an approximate expression can be derived for the critical flux, namely,

$$\Phi_c \approx 4\kappa_c^2 \gamma_0 D_0 k^2 / \gamma_{nl}^2. \tag{22}$$

In real units the critical thermal flux is of the order of $nD_0\kappa_c(kl)^2$, where n is the density. It is found that the solution is ballistic for equilibrium heat fluxes smaller than this critical value. These are situations where the temperature gradient is close to the threshold. Sharp fronts (meaning high wave numbers) satisfy this condition more easily than smooth structures. Hence it is expected that for a fixed thermal flux, a sharp front propagates ballistically, while a large scale thermal wave behaves diffusively.

IV. SELF-SIMILAR FRONTS

A. Scale invariance

Self-similar fronts have a long story which traces back (at least) to Anderson and Lysak[28] in the context of fusion plasmas. It was shown recently by Hahm *et al.*[16] that Eq. (2) admits self-similar solutions at fixed growth rate, i.e., at fixed temperature gradient with the present notations. It appears

quite natural to extend this result to the system Eqs. (1) and (2). Self-similar solutions are investigated by looking for the transformations

$$x \to \alpha_x x, \quad t \to \alpha_t t, \quad T \to \alpha_T T, \quad E \to \alpha_E E, \tag{23}$$

that leave the system invariant. It appears readily that $\alpha_T = \alpha_x/\alpha_t$ and $\alpha_E = \alpha_x^2/\alpha_t$. This solution holds provided that $\kappa_c = 0$ (situation well above the threshold), and $\gamma_{nl} = 0$, i.e., the system saturates via profile relaxation and/or turbulence spreading. The system to be solved reads

$$\partial_t T = D_0 \partial_x (E \partial_x T), \tag{24}$$

$$\partial_t E = \gamma_0 E \partial_x T + D_1 \partial_x (E \partial_x E). \tag{25}$$

This system is invariant by translation, which implies that space and time coordinates can be arbitrarily shifted by a constant, i.e., $x \to x - x_0$ and $t \to t - t_0$. To simplify the analysis we assume an infinite medium. We add an additional constraint of energy conservation, i.e., $\int dx T$ is required to be conserved during the front propagation. This additional constraint comes from the conservative nature of the heat equation, which imposes that $\partial_t \int dx T = 0$ if the turbulent heat flux $E\partial_x T$ vanishes at infinity. This constraint imposes that $\alpha_x^2 = \alpha_t$. It is also the unique acceptable scaling when a background diffusion is accounted for. Finally the number of parameters can be reduced by normalizing the spatial and time coordinates, namely, $x \to \sqrt{\gamma_0/D_0}\, x$ and $t \to \gamma_0 t$. Combining the change of variables afore mentioned, and this new constraint, the temperature and the turbulence intensity can be formulated as

$$T = \frac{D_0}{\gamma_0 [D_0 (t - t_0)]^{1/2}} \mathcal{T}\left\{ \frac{x - x_0}{[D_0 (t - t_0)]^{1/2}} \right\},$$
$$E = \mathcal{E}\left\{ \frac{x - x_0}{[D_0 (t - t_0)]^{1/2}} \right\}. \tag{26}$$

These expressions are valid for $t > t_0$. They can be extended to the domain $t < t_0$ by using the symmetry rules (23) with $\alpha_t = -1$ (details are given in the next section). Note also that the temperature can be shifted by any arbitrary constant, but not the intensity. Imposing vanishing front amplitudes $\mathcal{E} = 0$ (or $\partial_u \mathcal{T} = 0$) and $\mathcal{T} = 0$ at one end of the front, it is found that the functions $\mathcal{T}$ and $\mathcal{E}$ are solutions of the following ordinary differential equations:

$$2\mathcal{E}\partial_u \mathcal{T} + u\mathcal{T} = 0,$$
$$u\partial_u \mathcal{E} + 2\partial_u \mathcal{T}\mathcal{E} + 2d_1 \partial_u (\mathcal{E}\partial_u \mathcal{E}) = 0, \tag{27}$$

where $d_1 = D_1/D_0$.

B. Solutions without turbulence spreading

We first address the case without spreading ($d_1 = 0$). A particular solution exists at $\mathcal{T} = -u$ and $\mathcal{E} = -u^2/2$, or equivalently

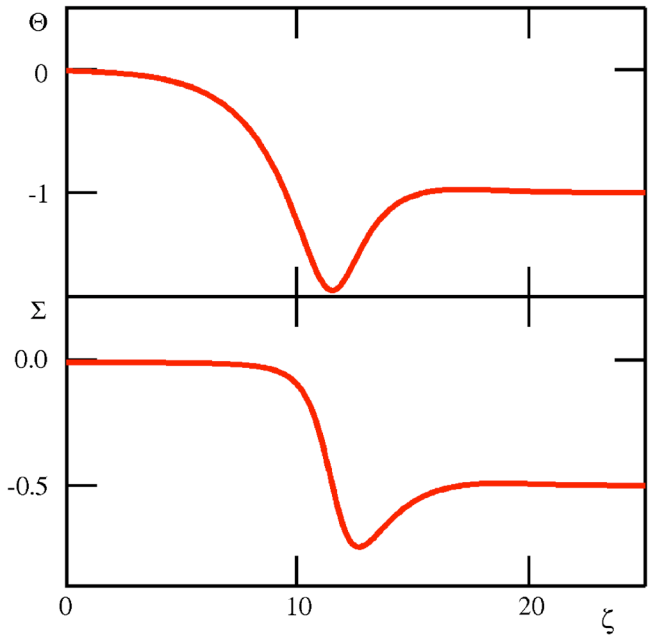

FIG. 1. (Color online) Self-similar front, $D_1 = 0$.

$$T = \frac{x - x_0}{\gamma_0 (t_0 - t)}, \quad E = \frac{(x - x_0)^2}{2D_0 (t_0 - t)}. \tag{28}$$

It can be verified directly from Eqs. (24) and (25) that this solution is in fact valid for all times. However it is only physically meaningful for $t < t_0$ since the turbulence intensity must be positive (the situation for the temperature is more complicated since it depends on the sign of $x - x_0$, and also it is defined up to an arbitrary constant). In fact, Eq. (28) is not a front since it does not link two different states of the plasma. Moreover it exhibits a finite time singularity at $t = t_0$. More physical solutions can be constructed using the following method. The system Eq. (27) for $d_1 = 0$ is shown in Appendix A to be equivalent to the following set of equations:

$$\partial_\zeta \Theta = \left(\Sigma + \tfrac{1}{2}\right)\Theta, \quad \partial_\zeta \Sigma = (2\Sigma - \Theta)\Sigma, \tag{29}$$

where $\mathcal{E} = u^2 \Sigma$ and $\mathcal{T} = u\Theta$, and the variable ζ is related to the variable u via the relation $du/u = -\Sigma d\zeta$. The system Eq. (29) is solved numerically by considering it as a dynamical system, where ζ plays the role of time. Two fixed points obviously exist: ($\Theta_I = 0$, $\Sigma_I = 0$), and ($\Theta_{II} = -1$, $\Sigma_{II} = -1/2$). The first point is unstable (more precisely it is neutrally stable along one direction and unstable along all the others), while the second fixed point is stable (see Appendix A for details). This stable point actually corresponds to the solution Eq. (28). "Trajectories" can be found, that link the first fixed point to the second one. These trajectories correspond to diffusive front solutions. An example is shown in Fig. 1, which is a self-similar front as a function of the "time" ζ. It is obtained by launching a trajectory that starts from the point I ($\Theta = 0$, $\Sigma = 0$), with a horizontal tangent, and ultimately reaches the point II ($\Theta_{II} = -1$, $\Sigma_{II} = -1/2$). The trajectory is shown in Fig. 2. Once the functions $\Theta(\zeta)$ and $\Sigma(\zeta)$ are known, their shape can be found as functions of the variable

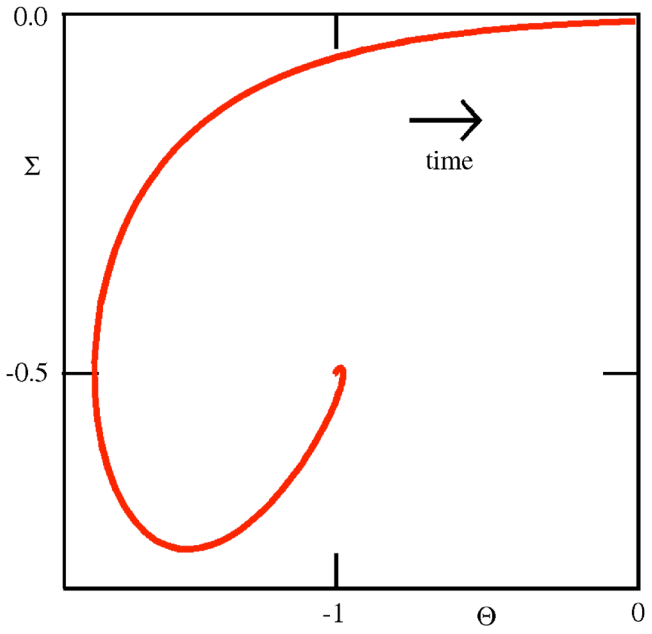

FIG. 2. (Color online) Trajectory of a self-similar front in phase space, $D_1=0$. The arrow shows the direction of time t. The variable ζ flows in the opposite direction, i.e., from the point I ($\Theta=0$, $\Sigma=0$), to the point II ($\Theta_{II}=-1$, $\Sigma_{II}=-1/2$).

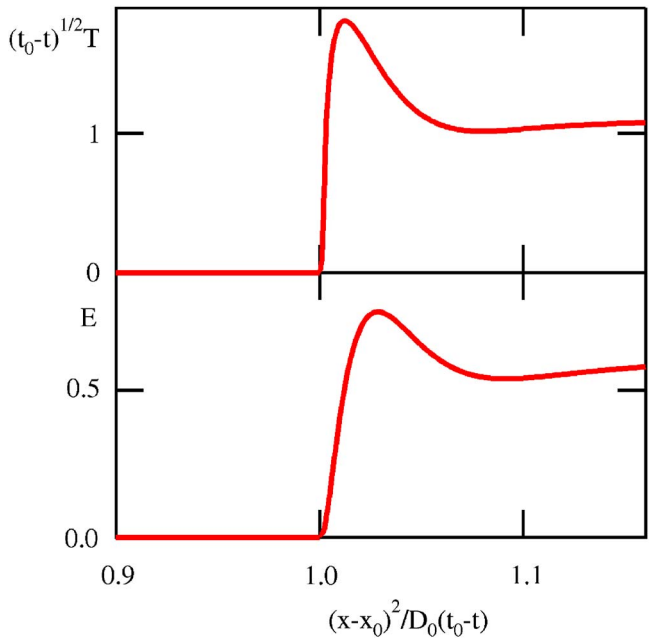

FIG. 3. (Color online) Self-similar diffusive front, $D_1=0$.

$$u=\frac{x-x_0}{[D_0\gamma_0(t-t_0)]^{1/2}},$$

using the change of variable $du/u=-\Sigma d\zeta$, i.e.,

$$u=u_0\exp\left[-\int_0^{\zeta}\Sigma(\zeta')d\zeta'\right]. \tag{30}$$

However, this reconstruction leads to negative turbulence intensities, which are not acceptable. Moreover, Eq. (30) shows that the variable

$$u=\frac{x-x_0}{[D_0\gamma_0(t-t_0)]^{1/2}}$$

increases with ζ since Σ is negative. Therefore the variables t and ζ flow in opposite directions. This implies that the front reaches the zero value for infinite time t. This is not what is searched for, as one would like the front to vanish when $t\to t_0$ to avoid a singularity at $t=t_0$. More physical solutions can be constructed by using the time reversal symmetry rule ($\alpha_t=-1$ and $\alpha_x=1$),

$$x\to x,\quad t\to -t,\quad T\to -T,\quad E\to -E. \tag{31}$$

This is done by expressing the functions $\mathcal{E}=u^2\Sigma$ and $\mathcal{T}=u\Theta$ as functions of u^2, then making the transform $u^2\to -u^2$, $E\to -E$, and $T\to -T$. It is interesting to recover the particular solution Eq. (28) when using this method. The fixed point II ($\Theta_{II}=-1$, $\Sigma_{II}=-1/2$) corresponds to the explicit solution $\mathcal{T}=-u$ and $\mathcal{E}=-u^2/2$. This solution is the same as Eq. (28), but with the restriction $t>t_0$ for the variable u to be meaningful. The symmetry rules (31) allow us to extend the solution to the domain $t<t_0$. In this particular case, this operation demonstrates that the solution Eq. (28) is in fact valid for all times [this can be verified directly from the initial system Eqs. (24) and (25)]. When applied to the example of Fig. 1, this technique leads to the solution shown in Fig. 3 (choosing $u_0=1$). This solution is defined for $t<t_0$. However it persists in exhibiting a finite time singularity at $t=t_0$. Although the time $t=t_0$ can be chosen to be arbitrarily large, this remains a pathological aspect of the solution. Finite size effects might cure this problem, but this question is beyond the scope of the present paper.

C. Self-similar fronts with turbulence spreading

Accounting for spreading does not raise any special difficulty, since the same procedure can be used. However the new system is somewhat more difficult to solve since the number of dynamical variables is higher. Indeed the system Eq. (29) is replaced by

$$\partial_\zeta\Theta=\left(\Sigma+\tfrac{1}{2}\right)\Theta,\quad \partial_\zeta\Sigma=\Sigma\Pi,$$
$$\partial_\zeta\Pi=-6\Sigma^2+7\Sigma\Pi-\Pi^2+\frac{1}{2d_1}(\Theta-2\Sigma+\Pi), \tag{32}$$

where the definitions of the functions and variables are the same as before. This system admits three fixed points:

$$\text{Fixed point I}\quad \Theta_I=0,\quad \Sigma_I=0,\quad \Pi_I=0;$$
$$\text{Fixed point II}\quad \Theta_{II}=-1+3d_1,\quad \Sigma_{II}=-\tfrac{1}{2},\quad \Pi_{II}=0; \tag{33}$$
$$\text{Fixed point III}\quad \Theta_{III}=0,\quad \Sigma_{III}=-\frac{1}{6d_1},\quad \Pi_{III}=0.$$

The stability analysis is done in Appendix A. It turns out that the first fixed point is always unstable (in fact one direction is neutrally stable and all the others are unstable). For $d_1<1/3$ the second fixed point is a saddle point, while the third fixed point is stable. Conversely when $d_1>1/3$, the second

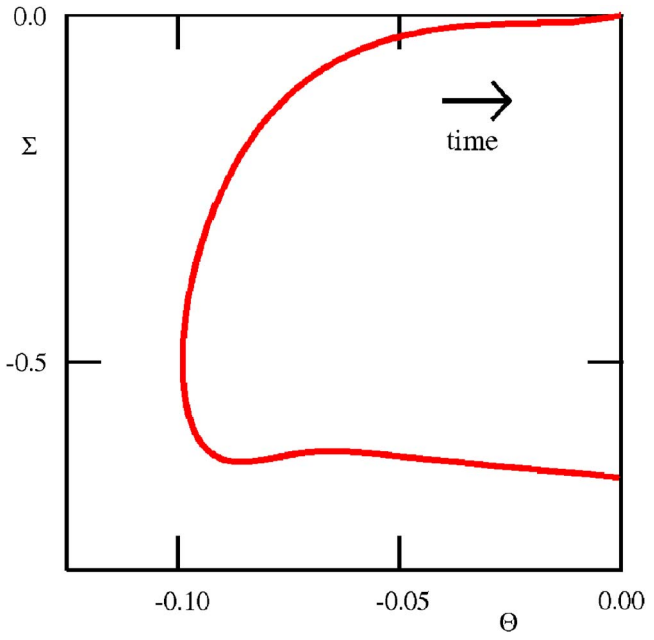

FIG. 4. (Color online) Trajectory of a self-similar front in phase space, with spreading ($D_1=0.25D_0$).

point is stable while the point III is a saddle point. Hence trajectories can be constructed, which link the first point to the third (respectively second) fixed point when $d_1<1/3$ (respectively $d_1>1/3$). An example of trajectory linking the fixed points I and III is shown in Fig. 4, and the corresponding front is drawn in Fig. 5 for $d_1=0.25$. The same procedure as in the previous section has been used to construct fronts with positive intensity. This trick cannot be used for $d_1>1/3$. The trajectories which are found in this case link the fixed point I to the fixed point II. As a consequence, their turbulence intensity is negative and the temperature positive.

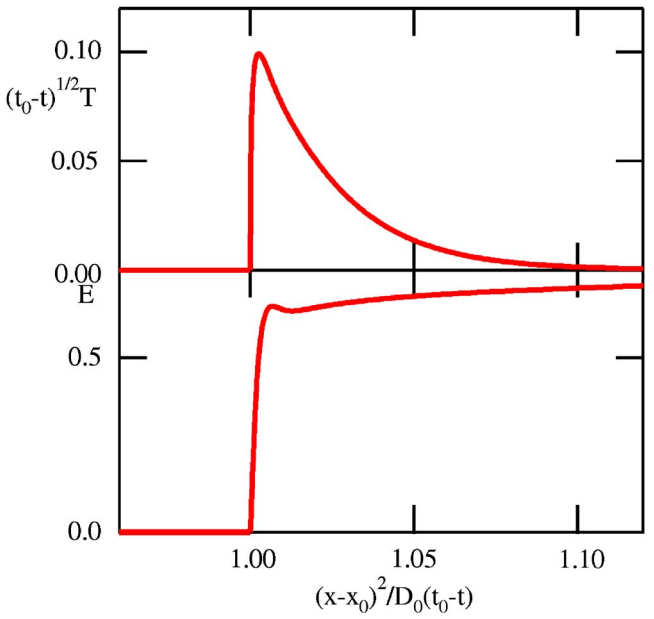

FIG. 5. (Color online) Self-similar diffusive front with spreading ($D_1=0.25D_0$).

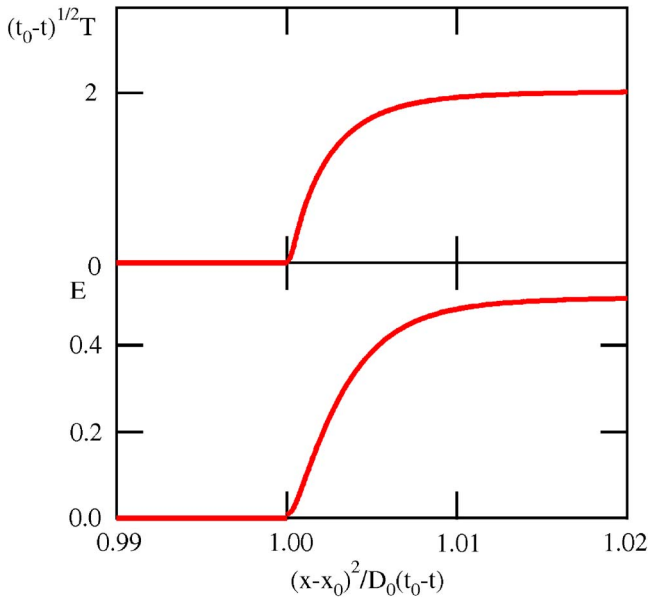

FIG. 6. (Color online) Self-similar diffusive front with spreading ($D_1=D_0$).

This difficulty is overcome by using the system invariance by central symmetry ($\alpha_t=-1$ and $\alpha_x=-1$), i.e.,

$$x \to -x, \quad t \to -t, \quad T \to T, \quad E \to -E. \tag{34}$$

The resulting front exhibits a positive intensity. An example is shown in Fig. 6 for $d_1=1$. Therefore acceptable self-similar solutions are found for all values of d_1. They nevertheless exhibit a finite time singularity as mentioned before. These solutions are in essence diffusive. Since they appear well above the threshold, they can be considered as the nonlinear version of the diffusive heat waves discussed previously. We note also that "conventional" diffusive pulses can be found by reversing the "time" ζ, and building trajectories which start from the now stable fixed point I and return to it. Note that a difference is made here between a "front," that relates two different states (i.e., two fixed points in the phase space), and "pulses," which are transients around a single state (a trivial example is illustrated by a simple diffusion equation). Regarding this question, we note that the present system is characterized by one stable state only. Results would certainly change for a bistable system, which would be found for instance when including a strong shear flow. In the latter case, nonlinear pulse solutions are also expected.

V. BALLISTIC FRONTS

A. Linear front selection

Ballistic fronts are solutions of the form $F(x-ct)$ connecting two states of the plasma, where F stands for the two fields T and E, and c is the front velocity. It is possible to use the linear dispersion relation derived in Sec. III to get a first idea of the characteristics of a front that moves into an unstable medium. The solutions which are found in this way are approximate, but this method enlightens the nonlinear results. Here we follow here closely the procedure described by Dee and Langer[29] (also see the overview by Cross and Hohenberg[30] and Diamond *et al.*[11] for an early application in

plasma physics). Expressing the leading edge of a front as a Fourier integral, its shape at a given position and time reads

$$F(x=ct,t)=\oint \frac{dk}{2\pi}F_k \exp\{i[kc-\omega(k)]t\}, \tag{35}$$

where $\omega(k)$ is a solution of the linear dispersion relation Eq. (15). The contour of integration is in the complex plane $k=q_L+i\kappa_L$, and the pulsation is also a complex number $\omega=\omega_r+i\omega_i$. Performing the integral by using a method of steepest descent, one finds the prescription for the wave number k^* that characterizes the front[29]

$$c=d_k\omega|_{k=k^*}. \tag{36}$$

Minimizing the damping of the front leads to a second condition

$$c=\frac{\omega_i(k^*)}{\kappa_L}. \tag{37}$$

These two relations have been interpreted in the following way by Van Saarlos.[31] The condition Eq. (36) leads to the following relation: $\mathrm{Im}(d_k\omega)=\partial_{q_L}\omega_i|_{\kappa_L}=0$. This constraint defines a relation linking q_L to κ_L, so that ω_r and ω_i can be considered now as a function of κ_L only, i.e., $\omega_{r,i}(\kappa_L)=\omega_{r,i}[q_L(\kappa_L),\kappa_L]$. Equation (37) then leads to the relation $c(\kappa_L)=\omega_i(\kappa_L)/\kappa_L$. Using now the real part of Eq. (36), it is readily shown that the speed of the front is the one that is minimal among the various values $c(\kappa_L)$, i.e., such that $\partial_{\kappa_L}c=0$. In other words, the most robust front is the slowest one. In summary the front speed is fully determined by three conditions, namely,

$$\partial_{q_L}\omega_i|_{\kappa_L}=0, \tag{38}$$

which relates q_L to κ_L, and

$$c(\kappa_L)=\omega_i(\kappa_L)/\kappa_L, \tag{39}$$

$$\partial_{\kappa_L}c=0. \tag{40}$$

This recipe is now applied to the two-field critical gradient model. It is quite important to note that this technique applies to a front that propagates into an unstable state. Hence the linear dispersion relation Eq. (16) must be applied for an arbitrary unstable state (A_0,E_0). It can be easily verified that $q_L=0$ is the solution of the equation $\partial_{q_L}\omega_i|_{\kappa_L}=0$. The relation $c(\kappa_L)=\omega_i(\kappa_L)/\kappa_L$ then yields an explicit equation for the speed of each front characterized by the wave number κ_L, namely,

$$c(\kappa_L)=\frac{1}{2}\left[\frac{\gamma}{\kappa_L}+(\mathcal{D}_1+\mathcal{D}_0)\kappa_L\right] \pm sg(\kappa_L)\left\{v_f^2+\frac{1}{4}\left[\frac{\gamma}{\kappa_L}+(\mathcal{D}_1-\mathcal{D}_0)\kappa_L\right]^2\right\}^{1/2}, \tag{41}$$

where $v_f=(D_0\gamma_0A_0E_0)^{1/2}$ and $\gamma=\gamma_0(A_0-\kappa_c)-2\gamma_{nl}E_0$ ($\gamma>0$ since the state is unstable). One has in principle to solve $\partial_{\kappa_L}c=0$ to find the front speed. However examining the structure of Eq. (41) leads to a typical scale of the front of the order of $(\mathcal{D}/\gamma)^{1/2}$, i.e., of the order of the correlation length of turbulence ($\mathcal{D}=\mathcal{D}_0+\mathcal{D}_1$). Two limit cases can be distinguished. If $\gamma\ll\gamma_0A_0$, the velocity v_f is much larger than $(\gamma\mathcal{D})^{1/2}$. The front speed exhibits a minimum for $\kappa_L\simeq(\gamma_{\mathrm{eff}}/\mathcal{D})^{1/2}$ so that $c(\kappa_L)\simeq v_f$. In the opposite case, one recovers the Fisher-Komogorov solution, i.e., $c(\kappa_L)=\frac{1}{2}(\gamma/\kappa_L+\mathcal{D}_1\kappa_L)$. The front typical wave number is $\kappa_L=(\gamma/\mathcal{D}_1)^{1/2}$, and the minimum speed appears to be $c=(\gamma\mathcal{D}_1)^{1/2}$. In fact, in all cases the front speed is the algebraic mean between the diffusion coefficient and the growth rate. This result has been extended to a fractional version of the Fisher-Kolmogorov equation.[32]

This analysis bears some drawbacks. The choice of the unstable state (A_0,E_0) is not constrained here. A natural choice would be the unstable fixed point $E_0=0$. However this is a somewhat ill-posed problem since in this case the turbulent diffusion coefficients $\mathcal{D}_0$ and $\mathcal{D}_1$ vanish, and the velocity v_f as well. This is why a detailed analysis of the nonlinear regime is required at this point.

B. Nonlinear ballistic solutions

We now turn to exact nonlinear ballistic solutions. For this analysis, it is easier to start from the system Eqs. (7) and (8). This question has already been investigated by Sarazin *et al.*[14] for a similar two-field system, where the coupling between the turbulent flux and the turbulent intensity was however different. Also analytical results have been provided by Gürcan and Diamond[23] for this very same two-field CGM model at fixed temperature gradient. They also solved numerically the dynamics of a perturbation for the complete system. For the case at fixed temperature gradient, the equation Eq. (8) is a variant of the Fisher-Kolmogorov equation, which admits ballistic front-like solutions. Here we focus the analysis on the case where fronts come from the interplay between the gradient relaxation via the transport equation coupled to the turbulent intensity dynamics. As mentioned before, we expect this kind of situation to occur at low heat flux, i.e., close to the threshold κ_c. To start with, we get rid of all kinds of mode coupling, including turbulence spreading, i.e., $\gamma_{nl}=0$ and $D_1=0$. The first step consists in choosing normalized coordinate $\rho=\sqrt{\gamma_0/D_0}x$ and time $\tau=\gamma_0t$, so that the system Eqs. (7) and (8) reads (far from the heat source location)

$$\partial_\tau A=\partial_{\rho\rho}(EA), \tag{42}$$

$$\partial_\tau E=(A-\kappa_c)E. \tag{43}$$

Looking for solutions of the form $A(\eta)$, $E(\eta)$, where $\eta=\tau-\rho/c$, one finds that

$$\partial_\eta(EA)=c^2(A-\kappa_c), \tag{44}$$

$$\partial_\eta E=(A-\kappa_c)E, \tag{45}$$

where a constant of integration has been chosen such that the marginal state $A=\kappa_c$ is a fixed point of the dynamical system. It is quite convenient to introduce the flux $\Gamma=EA$ as an auxiliary function. It appears readily that $E\exp(-\Gamma/c^2)$ is a first integral of the system. The formal solution of Eqs. (44) and (45) is

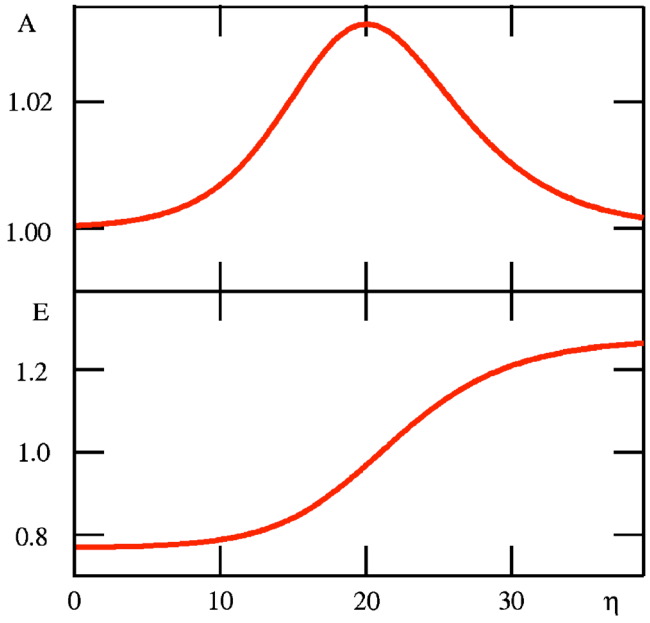

FIG. 7. (Color online) Ballistic front $\kappa_c=1$, $E_f=1$, and $\varepsilon=0.25$.

$$\eta=\frac{E_f}{c^2}\int^{\Gamma}\frac{d\Gamma}{\Gamma\exp\left(-\frac{\Gamma}{c^2}+1\right)-E_f\kappa_c}, \tag{46}$$

$$E=E_f\exp\left(\frac{\Gamma}{c^2}-1\right), \tag{47}$$

$$A=\frac{\Gamma}{E_f}\exp\left(-\frac{\Gamma}{c^2}+1\right), \tag{48}$$

where E_f is a reference value, which corresponds to $\Gamma=c^2$. The reason for this normalization is that the denominator under the integral in Eq. (46) is minimum when $\Gamma=c^2$. A front solution exists if this denominator admits 2 zeros on each side of $\Gamma=c^2$. This situation occurs if $E_f\kappa_c\le c^2$. An explicit solution can be found when $E_f\kappa_c/c^2$ is close to one. Introducing the parameters

$$\varepsilon=\left[2\left(1-\frac{E_f\kappa_c}{c^2}\right)\right]^{1/2},\quad \alpha=\kappa_c\frac{\sqrt{\varepsilon/2}}{1-\varepsilon^2} \tag{49}$$

one finds that for $\varepsilon\ll 1$,

$$\Gamma=c^2[1+\varepsilon\tanh(\alpha\eta)],\quad E=E_f\exp[\varepsilon\tanh(\alpha\eta)],$$
$$A=\kappa_c\frac{1-\frac{\varepsilon^2}{2}\tanh^2(\alpha\eta)}{1-\frac{\varepsilon^2}{2}}. \tag{50}$$

The turbulence intensity exhibits a front structure and ranges between $E_f(1-\varepsilon)$ and $E_f(1+\varepsilon)$. The shape of the temperature gradient is rather a pulse, whose background corresponds to a marginal state $A=\kappa_c$ and exhibits a maximum at $A=\kappa_c/(1-\varepsilon^2/2)$. An example is shown in Fig. 7. As usual for this type of system, the front velocity c is related to the turbulence intensity E_f. According to the selection rule based on the leading edge stability, the most stable front is the slowest one, i.e., such that $c^2=E_f\kappa_c$. Given the normalization, the order of magnitude of this speed in real units is $\sqrt{D_0E_f\gamma_0\kappa_c}$, i.e., is identical to the front velocity found in Sec. V A, Eq. (41) when the gradient is close to the threshold $A_0\simeq\kappa_c$ and $E_0=E_f$. This scaling reflects the interplay between the profile relaxation and turbulence dynamics. It is obviously related to the dynamics of avalanches, as explained by Sarazin *et al.*[14]

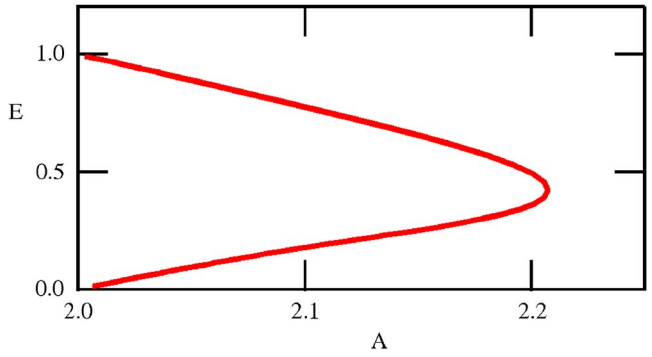

FIG. 8. (Color online) Trajectory in the phase space for the system Eq. (52) $\kappa_c=1$, $A_\star=2$, $\kappa_c=1$, $D_1=D_0$, and $c=2$.

The general case corresponds to the system Eqs. (7) and (8), and in order to make the connection with the work of Gürcan and Diamond,[23] we choose to normalize the system to a radius $\rho=\sqrt{\gamma_0/D_1}x$ and time $\tau=\gamma_0 t$, i.e.,

$$\partial_\tau A=d_0\partial_{\rho\rho}(EA),\quad \partial_\tau E=(A-\kappa_c)E-gE^2+\partial_\rho(E\partial_\rho E), \tag{51}$$

where $g=\gamma_{nl}/\gamma_0$ and $d_0=D_0/D_1$. Ballistic front solutions of Eq. (51) correspond to functions that depend on the variable $\eta=\tau-\rho/c$ only. It is quite useful to introduce the auxiliary function F, defined as the derivative of E with respect to η, i.e., $F=\partial_\eta E$. The resulting equations exhibit a singularity at $E=0$, which can be removed by introducing the variable ζ such as $\partial_\zeta=-E\partial_\eta$. The functions $A(\zeta)$, $E(\zeta)$, and $F(\zeta)$ are found to be solutions of the autonomous system

$$\partial_\zeta A=-\frac{c^2}{d_0}(A-A_\star)+AF,\quad \partial_\zeta E=-EF,$$
$$\partial_\zeta F=F^2-c^2[F-(A-\kappa_c)E+gE^2]. \tag{52}$$

The dynamical system Eqs. (52) admits three fixed points

$$\text{Fixed point I}\quad A_{\rm I}=A_\star,\quad E_{\rm I}=0,\quad F_{\rm I}=0;$$
$$\text{Fixed point II}\quad A_{\rm II}=-\frac{1}{1-d_0}A_\star,\quad E_{\rm II}=0,\quad F_{\rm II}=c^2; \tag{53}$$
$$\text{Fixed point III}\quad A_{\rm III}=A_\star\quad E_{\rm III}=E_\star=\frac{A_\star-\kappa_c}{g}\quad F_{\rm III}=0.$$

The stability of these fixed points is discussed in Appendix B. The fixed point I is stable, while the two others are saddle points. Fronts can be built by linking a saddle point to another saddle point, or by linking a saddle point to the stable fixed point I, depending on the parameters. These "trajecto-

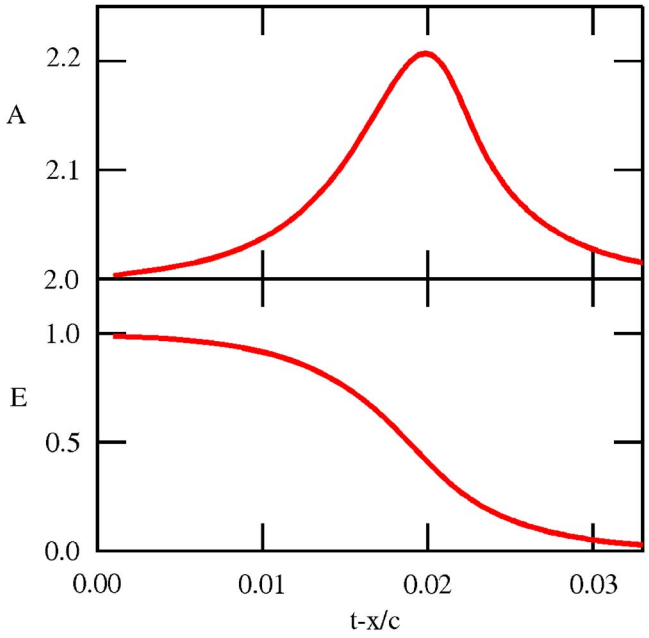

FIG. 9. (Color online) Ballistic front or the system Eq. (52) $\kappa_c=1$, $A_\star=2$, $\kappa_c=1$, $D_1=D_0$, and $c=2$.

ries" cover both the class of solutions described above and the previous work by Gürcan and Diamond.[23] The Fisher-Kolmogorov equation corresponds to the limit $d_0=0$. In practice, trajectories linking fixed points, namely fronts, are found in a large domain of parameters. An example is given in Fig. 8 (fixed point III to fixed point I) and the corresponding front is shown in Fig. 9. Also it is found numerically that for a given set of parameters fronts do not exist below some critical value of the speed c. Following the selection rule mentioned before, this lowest velocity is the speed of the most robust (meaning less damped) front. In real units it always scales as the algebraic mean of the diffusion coefficient and growth rate. It is quite remarkable that adding spreading and mode coupling does not change the scaling of the front velocity. In fact this can be understood in view of the process of linear front selection as discussed in Sec. V A. As the front speed results from a balance between the linear growth rate and some turbulent diffusion, it is quite insensitive to the details of the various nonlinear processes which are involved. We note also that the front speed can be quite low when the gradient is close to the threshold, i.e., at low heat flux.

VI. DISCUSSION

This paper presents some dynamical properties of a two-field critical gradient model, which connects a turbulent transport equation to an evolution equation for the turbulence intensity. The dynamics of the turbulence intensity is characterized by an exponential growth above a stability threshold, a quadratic saturation term, and a turbulence spreading component. It is shown here that this model exhibits both diffusive and ballistic behaviors. This can be verified by analyzing the linear response of this system. More precisely, a diffusive response is obtained when the temperature gradient is well above the stability threshold, and also when the perturbation is characterized by large spatial scales. Conversely, thermal waves that propagate ballistically are found when the temperature gradient is close to the threshold, and also for perturbations that exhibit small spatial scales. The condition for switching from ballistic to diffusive dynamics can be expressed as a constraint on the thermal flux versus the typical wave number k of the pulse. Ballistic propagation is found when the thermal flux is smaller than $nD_0\kappa_c(k\ell)^2$, where n is the density, κ_c is the critical temperature gradient, D_0 a typical (mixing-length) turbulent diffusion coefficient, and ℓ a turbulence correlation length. This result is valid if the pulse length scale is larger than the turbulence correlation length (i.e., $k\ell<1$), which is also a condition for using a mean field model. The ballistic behavior comes from the interplay between the profile relaxation due to turbulence, and the growth of turbulence intensity due to profile steepening. This mechanism is the same as the one described previously for avalanching.[14] As mentioned before in this context, a system will be prone to ballistic propagation if it is stiff. Also ballistic propagation may be related to the question of gyro-Bohm versus Bohm scaling law of confinement. One would expect the system to be sensitive to the plasma size when ballistic fronts are present. On this basis, a Bohm scaling would thus be expected at low heat power.

The ability of a two-field critical gradient model to behave diffusively or ballistically is a robust property. In fact this behavior is found to persist in the nonlinear regime. A manifestation of this robustness is the rich dynamics of fronts that has been found. Fronts are defined here as perturbation linking two different states of the plasma, for instance turbulent and nonturbulent states. It is found that both diffusive self-similar and ballistic fronts exist for a two-field critical gradient system.

Self-similar fronts are diffusive in nature. The diffusion coefficient that rules the dynamics of these fronts is the turbulent one. However self-similar diffusive fronts are not generic for this particular two-field critical model. They require the system to be well above the threshold, a condition reminiscent of the linear analysis. Also their existence relies on a vanishing saturating quadratic term in the evolution equation for the turbulence intensity. In other words, the dominant nonlinear linearities have to be the interplay between the turbulence growth and profile relaxation on the one hand, and turbulence spreading on the other hand. Finally these solutions exhibit a finite time singularity that is not physical, but might be prevented by finite size effect.

Ballistic fronts are a generic feature of a two-field critical gradient model. Two mechanisms exist in fact. The first one appears in the equation for the turbulence intensity alone, i.e., for frozen temperature gradient, and combines turbulence spreading, exponential growth and quadratic saturation. This equation is a variant of the Fisher-Kolmogorov equation that describes reaction-diffusion processes, and has been extensively studied in the past.[23] The second mechanism is an avalanche-like process that combines profile relaxation and exponential growth. The speed and radial scale of ballistic fronts can be derived by analyzing the linear stability of the front leading edge.[31] Indeed the most robust

front, meaning the one that is marginally stable, is the slowest one. Applying this rule to the present model, it is found that the front speed is the quadratic average of the instability growth rate and turbulent diffusion coefficient, $v_f=(\gamma D)^{1/2}$. A study of the nonlinear regime confirms this finding. It is found numerically that a minimum of the front speed exists and that it is of the order of v_f. This scaling remains valid when combining both mechanisms, avalanche-like and Fisher-Kolmogorov-type. It is also found that the radial scale of a fronts is of the order of $(D/\gamma)^{1/2}$, i.e., of the order of a few turbulence correlation lengths.

In a tokamak plasma, the velocity v_f scales as the diamagnetic velocity, i.e., is of the order of 100–1000 m s^{-1} for usual conditions. We note however that it can be smaller when the temperature gradient is close to the threshold. Hence a ballistic front will propagate faster than a diffusive one, since the turbulent diffusion coefficient is of the order of a few m^2 s^{-1}. At this stage, one may try a tentative interpretation of the observation of "slow" and "fast" transients in JET plasmas, where a slow transient would correspond to heat modulation (as it is well described by a one-field CGM model), while a fast transient would corresponds to a cold pulse triggered by impurity injection. Since the background plasma is the same for both experiments, one cannot argue about the distance to the threshold or on stiffness. On the other hand, it might be possible that a thermal wave triggered by a heat modulation using rf heating exhibits large spatial scales, whereas a cold pulse produced by impurity injection is likely sharper, sharp enough to enter the ballistic regime. Independent of these rather speculative arguments, the present study certainly shows that a model based on ordinary differential equations, may lead to diffusive or ballistic behaviors, which is in itself an interesting result. An open question though is whether this dual character persists when the effect of shear flow is included. This question is related to the problem of front propagation through a transport barrier. It is also linked to the issue of barrier formation via front propagation, which has already been addressed elsewhere with similar results.[11,35]

VII. CONCLUSION

This paper shows that a two-field critical gradient model that couples a heat equation to an evolution equation for turbulence intensity exhibits the characteristics of both diffusive and ballistic dynamics. This property becomes apparent when analyzing the linear response of this system for a heat wave, which is diffusive or ballistic depending on plasma parameters and wave number. More precisely diffusion is found when the background heat flux is high enough for the temperature gradient to largely exceed the threshold, while ballistic behavior is more prominent close to a marginal state. Also a sharp pulse propagates ballistically while a smoother one diffuses. This dual character is recovered when investigating the nonlinear solutions of this system. Self-similar diffusive fronts exist when the gradient is well above the threshold. The effective diffusion coefficient for propagation is of the order of the steady turbulent diffusivity. Hence self-similar diffusive fronts evolve slowly. Ballistic fronts have also been found, which propagate much faster. The front velocity is of the order of the quadratic mean of the turbulent diffusion coefficient and a typical instability growth rate. In a tokamak, this corresponds to a velocity of the order of a diamagnetic velocity, i.e., of the order of 100–1000 m s^{-1}. There is no precise recipe for switching from one solution to the other. However, the general trend is that self-similar diffusive fronts appear at large fluxes (well above the threshold), while ballistic fronts are characterized by a broader domain of existence. Ballistic fronts due to the interplay between profile relaxation and turbulence intensity dynamics appear close to the stability threshold. Thus the nonlinear results are consistent with the linear analysis. Hence it can be concluded that the dual character of a two-field critical gradient model is a robust feature, which might explain why the same physical system exhibits both slow diffusive and fast ballistic transport transients.

ACKNOWLEDGMENTS

This work was initiated at the Festival of Theory in Aix-en Provence 2005 and finalized during the 2007 edition. We thank Dr. D. F. Escande, Dr. T. S. Hahm, and Dr. V. Naulin for fruitful discussions.

APPENDIX A: SELF-SIMILAR FRONTS

We consider here the system Eq. (27), assuming in a first stage $d_1=0$. An alternative form is

$$2\mathcal{E}\partial_u\mathcal{T}=-u\mathcal{T},\quad \partial_u\mathcal{E}=\mathcal{T}. \tag{A1}$$

One can use the usual sequence of tricks for solving a set of nonlinear differential equations. First, the explicit dependence on the variable u can be reduced by performing the change of functions[33] $\mathcal{E}=u^2\Sigma$ and $\mathcal{T}=u\Theta$, a consequence (again) of scale invariance. This procedure leads to the new system

$$2\Sigma(u\partial_u\Theta+\Theta)+\Theta=0,\quad u\partial_u\Sigma+2\Sigma-\Theta=0. \tag{A2}$$

The new system is equidimensional in the variable u (i.e., it is invariant when changing u in au, where a is a constant). Hence the explicit dependence on u can be eliminated via the change of variable $u=e^{-v}$,[33] i.e.,

$$2\Sigma\partial_v\Theta=(2\Sigma+1)\Theta,\quad \partial_v\Sigma=2\Sigma-\Theta. \tag{A3}$$

The new system is autonomous, i.e., no longer depends on the variable v. Nevertheless it exhibits a singularity at $\Sigma=0$ which is difficult to deal with. It corresponds to a physical situation where turbulence is suppressed. This technical difficulty is overcome by performing a new change of variable such that $\partial_\zeta=\Sigma\partial_v$,[34] which yields the tractable system Eq. (29). This system can be treated in the usual way, i.e., by considering it as a set of equations defining trajectories in the space (Θ,Σ), with the variable ζ playing the role of time.[34,30] There is no motion invariant for this system. Nevertheless, its behavior can be determined by looking at the stability of the fixed points. Two fixed points are readily found: $(\Theta_I=0,\ \Sigma_I=0)$, and $(\Theta_{II}=-1,\ \Sigma_{II}=-1/2)$. Their stability is investigated by calculating the eigenvalues of the tangent matrix: a positive real part of an eigenvalue corresponds to a

"repulsive" direction determined by the corresponding eigenvector, i.e., the trajectory moves away from the fixed point along this line, while a negative real part corresponds to an attractive direction. If all directions are attractive, the fixed point is stable, while it is unstable if all directions are repulsive. For the present system, the tangent matrix reads as

$$M = \begin{pmatrix} \Sigma + \frac{1}{2} & \Theta \\ -\Sigma & -\Theta + 4\Sigma \end{pmatrix}. \tag{A4}$$

It is easily found that the first fixed point ($\Theta_I=0$, $\Sigma_I=0$) is characterized by a neutral direction along the Σ axis (corresponding to the eigenvalue) $\lambda_-=0$ and an unstable direction along the Θ axis ($\lambda_-=1/2$). Hence it is essentially an unstable fixed point. The second fixed point ($\Theta_{II}=-1$, $\Sigma_{II}=-1/2$) is stable $\left(\lambda_\pm=-\frac{1}{2}\pm\frac{i}{2}\right)$ and corresponds to the particular solution presented previously. We note that the direction of "time" ζ is arbitrary, i.e., when changing ζ in $-\zeta$, an attractive direction becomes repulsive and vice versa. Hence for a trajectory $I\rightarrow II$, there exists a trajectory $II\rightarrow I$ obtained via time reversal. With the present convention, trajectories can be built, which link the unstable fixed point I to the stable fixed point II. An example is shown on Figs. 1–3.

Adding turbulence spreading does not present any special difficulty, except that it increases the order of the system. The sequence of changes of functions and variables is the same and will not be repeated here. The system Eq. (29) is replaced by Eq. (32). As expected, the previous system Eq. (29) is recovered when $d_1=0$. This system admits three fixed points given by Eq. (33). We note that the fixed points II and III coalesce when $d_1=1/3$. The procedure is the same as previously, i.e., identifying the stability of the fixed points. The success of the procedure is however not guaranteed for a 3D system, in contrast to 2D systems. Using the fact that all three fixed points are such that $\Pi=0$, the tangent matrix for the system of coordinates (Θ,Σ,Π) is

$$M = \begin{pmatrix} \Sigma + \frac{1}{2} & \Theta & 0 \\ 0 & 0 & \Sigma \\ \frac{1}{2d_1} & -12\Sigma - \frac{1}{d_1} & 7\Sigma + \frac{1}{2d_1} \end{pmatrix}. \tag{A5}$$

For the fixed point I, the tangent matrix admits three eigenvalues 0, $\frac{1}{2}$, and $\frac{1}{2d_1}$. Hence it is unstable in two directions, and neutrally stable along the Σ axis.

For the fixed point II, the eigenvalues are solutions of the equation

$$\lambda^3 + \left(\frac{7}{2} - \frac{1}{2d_1}\right)\lambda^2 + \left(3 - \frac{1}{2d_1}\right)\lambda + \frac{3}{4} - \frac{1}{4d_1} = 0. \tag{A6}$$

An interesting limit case corresponds to $d_1\rightarrow 0$, which makes the connection with the previous analysis. One finds that a large positive eigenvalue $\lambda_0\simeq 1/2d_1$ and a couple of eigenvalues with a negative real part $\lambda_\pm\simeq -\frac{1}{2}\pm i$. One direction is repulsive while the other two are attractive. For the other values of d_1, a numerical analysis shows that there is always an unstable direction for $d_1<1/3$, while all directions are attractive for $d_1>1/3$. The second fixed point is stable when $d_1>1/3$.

Finally, for the fixed point III, the eigenvalues are solutions of the equation

$$\left(\lambda - \frac{1}{2} + \frac{1}{6d_1}\right)\left(\lambda^2 + \frac{2}{3d_1}\lambda + \frac{1}{6d_1^2}\right) = 0. \tag{A7}$$

This system admits three solutions $\lambda_0=\frac{1}{2}-(1/6d_1)$, and $\lambda_\pm=-(1/3d_1)[1\pm(i/\sqrt{2})]$. As expected, for $d_1=1/3$ the eigenvalues of points II and III are identical, i.e., $\lambda_0=0$, $\lambda_\pm=-1\mp(i/\sqrt{2})$. If $d_1<1/3$, the real parts of all the s are negative. In this case, the fixed point III is stable. For $d_1>1/3$ one direction is unstable and it becomes a saddle point. The fixed point III (resp. II) provides an exact analytical solution when $d_1<1/3$ (resp. $d_1>1/3$), similar to Eq. (28). However these solutions are not acceptable since they are singular when $t=t_0$. Acceptable solutions can be constructed by considering trajectories which start from the unstable fixed point I, and reaches the fixed point III for $d_1<1/3$ or the fixed point II for $d_1>1/3$. As mentioned before, the success of this construction is not guaranteed. However both types of fronts are indeed found numerically when using this recipe. An example is shown in Fig. 5. It is stressed that the nature of the fronts is different from the case without spreading when $d_1<1/3$ since the temperature difference goes back to zero, i.e., exhibits a pulse shape rather than a front shape. The corresponding trajectory is shown in Fig. 4.

APPENDIX B: BALLISTIC FRONTS

We start from the system Eqs. (52). The method for analyzing this system is the same as in Appendix A. The dynamical system Eqs. (52) admits 3 fixed points Eqs. (53). The tangent matrix for the "trajectory coordinates" (A,E,F) is

$$M = \begin{pmatrix} F - \frac{c^2}{d_0} & 0 & A \\ 0 & -F & -E \\ c^2E & c^2[(A-\kappa_c) - 2gE] & 2F - c^2 \end{pmatrix}. \tag{B1}$$

The fixed point I is characterized by 3 eigenvalues $-(c^2/d_0)$, 0, and $-c^2$. Hence it is stable along all directions except one line along which it is neutrally stable. The tangent matrix of the second fixed point admits 3 eigenvalues $-[(1/d_0)-1]c^2$, $-c^2$, and c^2. Hence, if $d_0<1$, two directions are attractive, whereas the third one is repulsive. In other words the second fixed point is a saddle point. Regarding the third fixed point, the eigenvalues of the tangent matrix are solutions of the equation

$$\lambda^3 + c^2\left(1 + \frac{1}{d_0}\right)\lambda^2 - c^2\left(\mu - \frac{c^2}{d_0}\right)\lambda - \frac{c^4}{d_0}gE_\star^2 = 0, \tag{B2}$$

where $\mu=E_\star(2A_\star-\kappa_c)$. Since the coefficients of this polynomial are real, zeros are either real or complex conjugate. In fact it can be easily verified that the 3 zeros are always real. It appears that all 3 eigenvalues cannot have simultaneously positive real parts since their sum is negative [equal to

$-c^2(1+1/d_0)]$. Moreover the product of the eigenvalues is equal to $c^4 g E_\star^2/d_0$, which is always positive. Hence two roots are negative and one is positive, which means that the third fixed point is a saddle point characterized by two stable and one unstable directions. An interesting limit case occurs when the product of the eigenvalues $c^4 g E_\star^2/d_0$ is small. This covers a broad range of situations: small front speed c, gradient close to the threshold, large thermal diffusion D_0, and/or small nonlinear mode coupling g. The solutions of Eq. (B2) are then approximately

$$\lambda_0 = -\frac{c^2 g E_\star^2}{d_0 \mu - c^2},$$
$$\lambda_\pm = -\frac{1}{2}\left(1+\frac{1}{d_0}\right)c^2 \pm \frac{1}{2}\sqrt{\left(1-\frac{1}{d_0}\right)^2 c^4 + 4\mu c^2}. \tag{B3}$$

Fronts can be built by linking a saddle point to another saddle point, or by linking a saddle point to the stable fixed point I. However we stress that not all solutions are possible for a given set of parameters. In particular, no fronts are usually found numerically for a speed c below a critical value. An example of trajectory tying the fixed point III to the fixed point I is shown in Fig. 8 and the corresponding front is shown in Fig. 9.

At this stage, it is possible to make the connection with previous works. The solution given in Sec. V corresponds to the case $g=0, d_1=0, A_\star=A_c$. Conversely the analytical solutions studied by Gürcan and Diamond[23] correspond to $d_0 \ll 1$ and a constant of integration $A_\star$ that is left free, but greater than κ_c. In this case, one recovers the Fisher-Kolmogorov equation and the eigenvalues read

$$\lambda_0 = \frac{c^2}{d_0}, \quad \lambda_\pm = -\frac{1}{2}\mu \pm \left\{\frac{1}{4}\mu^2 + c^2 g E_\star^2\right\}^{1/2}. \tag{B4}$$

Solutions exist, which connect the fixed point III to the fixed point I or to the fixed point II. This study will not be repeated here and can be found in Ref. 34. For $d_0=0$, a particular explicit solution can be found such that $F=c^2(1-E/E_\star)$ and $c^2=\frac{1}{2}gE_\star^2$ namely,

$$E = E_\star\left[1-\exp\left(-\frac{c^2\eta}{E_\star}\right)\right] \quad \text{for } \eta \geq 0$$
$$E = 0 \quad \text{for } \eta \leq 0. \tag{B5}$$

The velocity of the front is

$$c = \frac{1}{\sqrt{2}}[\gamma_0(A_\star - A_c)D_1 E_\star]^{1/2},$$

i.e., scales as a diamagnetic velocity in a tokamak plasma.

[1] H. Nordman, J. Weiland, and A. Jarmen, Nucl. Fusion **30**, 983 (1990); J. Weiland, "Collective Modes in Inhomogeneous Plasmas," IOP, 2000.
[2] R. E. Waltz, G. M. Staebler, W. Dorland, G. W. Hammett, M. Kotschenreuther, and J. A. Konings, Phys. Plasmas **4**, 2482 (1997).
[3] ITER Physics Expert Groups on Confinement and Transport and Confinement Modelling and Database, Nucl. Fusion **39**, 2175 (2000).
[4] P. Mantica and F. Ryter, C. R. Phys. **7**, 634 (2006).
[5] F. Imbeaux, F. Ryter, and X. Garbet, Plasma Phys. Controlled Fusion **43**, 1503 (2001).
[6] F. Imbeaux and X. Garbet, Plasma Phys. Controlled Fusion **44**, 1425 (2002).
[7] X. Garbet, P. Mantica, F. Ryter, G. Cordey, F. Imbeaux, C. Sozzi, A. Asp, V. Parail, R. Wolf, and the JET EFDA Contributors, Plasma Phys. Controlled Fusion **46**, 1351 (2004); **47**, 957 (2005) Addendum.
[8] F. Ryter, C. Angioni, A. G. Peeters, F. Leuterer, H.-U. Fahrbach, and W. Suttrop ASDEX Upgrade Team, Phys. Rev. Lett. **95**, 085001 (2005).
[9] P. Mantica, I. Coffey, R. Dux, X. Garbet, L. Garzotti, G. Gorini, F. Imbeaux, E. Joffrin, J. Kinsey, M. Mantsinen, R. Mooney, V. Parail, Y. Sarazin, C. Sozzi, W. Suttrop, G. Tardini, D. Van Eester, and JET EFDA Contributors, in *Proceedings of the 19th International Conference on Fusion Energy*, Lyon, 2002 (IAEA, Vienna, 2002), EX/P1-04.
[10] B. Ph. van Milligen, R. Sanchez, and B. A. Carreras, Phys. Plasmas **11**, 2272 (2004).
[11] P. H. Diamond, V. B. Lebedev, D. E. Newman, and B. A. Carreras, Phys. Plasmas **2**, 3685 (1995).
[12] D. E. Newman, B. A. Carreras, P. H. Diamond, and T. S. Hahm, Phys. Plasmas **3**, 1858 (1996).
[13] G. M. Staebler, R. E. Waltz, and J. C. Wiley, Nucl. Fusion **37**, 287 (1997)
[14] Y. Sarazin, X. Garbet, P. Ghendrih, and S. Benkadda, Phys. Plasmas **7**, 1085 (2000).
[15] V. Tangri, A. Das, P. K. Kaw, and R. Singh, Phys. Rev. Lett. **91**, 025001 (2003).
[16] T. S. Hahm, P. H. Diamond, Z. Lin, K. Itoh, and S-I. Itoh, Plasma Phys. Controlled Fusion **46**, A323 (2004).
[17] Ö. D. Gürcan, P. H. Diamond, T. S. Hahm, and Z. Lin, Phys. Plasmas **12**, 032303 (2005).
[18] R. E. Waltz and J. Candy, Phys. Plasmas **12**, 072303 (2005).
[19] V. Naulin, A. H. Nielsen, and J. Juul Rasmussen, Phys. Plasmas **12**, 122306 (2005).
[20] Ö. D. Gürcan, P. H. Diamond, and T. S. Hahm, Phys. Rev. Lett. **97**, 024502 (2006).
[21] J. Juul Rasmussen, V. Naulin, P. Mantica, J. S. Lönnroth, V. Parail, and JET-EFDA Contributors, in *Proceedings of the 33rd EPS Conference on Plasma Physics*, Rome, 19–23 June 2006 ECA, Vol. 30I, p. 1.076.
[22] X. Garbet, L. Laurent, A. Samain, and J. Chinardet, Nucl. Fusion **34**, 963 (1994).
[23] Ö. D. Gürcan, P. H. Diamond, and T. S. Hahm, Phys. Plasmas **14**, 055902 (2007).
[24] P. H. Diamond and T. S. Hahm, Phys. Plasmas **2**, 3640 (1995).
[25] B. A. Carreras, D. Newman, V. E. Lynch, and P. H. Diamond, Phys. Plasmas **3**, 2903 (1996).
[26] X. Garbet, Y. Sarazin, P. Beyer, P. Ghendrih, R. E. Waltz, M. Ottaviani, and S. Benkadda, Nucl. Fusion **39**, 2063 (1999).
[27] P. Beyer, S. Benkadda, X. Garbet, and P. H. Diamond, Phys. Rev. Lett. **85**, 4892 (2000).
[28] D. Anderson and M. Lisak, Phys. Rev. A **22**, 2761 (1980).
[29] G. Dee and J. S. Langer, Phys. Rev. Lett. **50**, 383 (1983).
[30] M. C. Cross and P. C. Hohenberg, Rev. Mod. Phys. **65**, 851 (1993).
[31] W. Van Saarlos, Phys. Rev. A **37**, 211 (1988); **39**, 6367 (1989).
[32] D. del-Castillo-Negrete, B. A. Carreras, and V. E. Lynch, Phys. Rev. Lett. **91**, 018302 (2003).
[33] C. M. Bender and S. A. Orszag, *Advanced Mathematical Methods for Scientists and Engineers* (McGraw-Hill, Singapore, 1978).
[34] J. D. Murray, *Mathematical Biology* (Springer, Berlin, 1991).
[35] D. del-Castillo-Negrete and B. A. Carreras, Phys. Plasmas **9**, 118 (2002).